Loss of phenotypic inheritance associated with *ydcI* mutation leads to increased frequency of small, slow persisters in *Escherichia coli*

Suzanne M. Hingley-Wilson[a,1], Nan Ma[a,b,1], Yin Hu[c,1], Rosalyn Casey[a], Anders Bramming[d], Richard J. Curry[e], Hongying Lilian Tang[c], Huihai Wu[a], Rachel E. Butler[a], William R. Jacobs Jr[f,g,3], Andrea Rocco[a,2,3], and Johnjoe McFadden[a,2,3]

[a]Department of Microbial and Cellular Sciences, School of Biosciences and Medicine, Faculty of Health and Medical Sciences, University of Surrey, Guildford GU2 7XH, United Kingdom; [b]Advanced Technology Institute, Department of Electronic Engineering, University of Surrey, Guildford GU2 7XH, United Kingdom; [c]Department of Computer Science, Faculty of Engineering and Physical Sciences, University of Surrey, Guildford GU2 7XH, United Kingdom; [d]Department of Forensic Medicine, University of Southern Denmark, DK-5320 Ribe, Denmark; [e]Photon Science Institute, Department of Electrical and Electronic Engineering, The University of Manchester, Manchester M13 9PL, United Kingdom; [f]Department of Microbiology and Immunology, Albert Einstein College of Medicine, Bronx, NY 10461; and [g]Department of Molecular Genetics, Albert Einstein College of Medicine, Bronx, NY 10461

Contributed by William R. Jacobs Jr, December 21, 2019 (sent for review September 6, 2019; reviewed by Bree B. Aldridge and Nathalie Q. Balaban)

Whenever a genetically homogenous population of bacterial cells is exposed to antibiotics, a tiny fraction of cells survives the treatment, the phenomenon known as bacterial persistence [G.L. Hobby *et al.*, *Exp. Biol. Med.* 50, 281–285 (1942); J. Bigger, *The Lancet* 244, 497–500 (1944)]. Despite its biomedical relevance, the origin of the phenomenon is still unknown, and as a rare, phenotypically resistant subpopulation, persisters are notoriously hard to study and define. Using computerized tracking we show that persisters are small at birth and slowly replicating. We also determine that the high-persister mutant strain of *Escherichia coli*, *HipQ*, is associated with the phenotype of reduced phenotypic inheritance (RPI). We identify the gene responsible for RPI, *ydcI*, which encodes a transcription factor, and propose a mechanism whereby loss of phenotypic inheritance causes increased frequency of persisters. These results provide insight into the generation and maintenance of phenotypic variation and provide potential targets for the development of therapeutic strategies that tackle persistence in bacterial infections.

persistence | antibiotic resistance | phenotypic | microbiology | systems biology

Antibiotic tolerance or persistence was first described by Hobby et al. in 1942 (1). Hobby observed that when a genetically homogenous *Streptococcus* culture was exposed to the bactericidal action of penicillin, a small number of cells [subsequently termed "persisters" by Bigger in 1944 (2)] survived the treatment. The phenomenon is an example of phenotypic variation as persisters are genetically identical to nonpersister cells. Persistence has been described in nearly all known microbes and is considered to be largely responsible for the resistance to antibiotic therapy of many chronic bacterial infections (3, 4).

Several features associate persistence to slow growth, such as their increased abundance in slowly growing (5) and stationary phase cells (6, 7). Classic microfluidic experiments in *Escherichia coli* demonstrated that persisters were slow-growing or nongrowing prior to antibiotic exposure (8). Two types of persisters were identified in this landmark publication: type I persisters that were mostly nongrowing cells formed during stationary phase and type II persisters that were mostly slow-growing cells generated during exponential growth. These have since been renamed in a consensus statement as triggered persistence or spontaneous persistence (i.e., generated during exponential or steady state growth) (9). Triggered persisters have been characterized particularly in the high-persister (Hip) A7 (*HipA7*) mutant strain of *E. coli*, whose phenotype is caused by a mutation in a gene encoding a toxin of a toxin–antitoxin system (10, 11). This has led to the proposal that stochastic expression of this gene causes triggered persistence (12). Spontaneous persisters are increased in the *HipQ* mutant strain (8), but the mechanisms by which these arise during steady state growth remain unknown as is the nature of the *HipQ* mutation. We recently proposed that persister cells correspond to the extreme slow end of the population distribution of growth rates associated with the phenotypic variation resulting from a variable expression of any growth rate-limiting gene (13).

Here we demonstrate that the high spontaneous persister mutant strain of *E. coli*, *HipQ*, is defective in its phenotypic inheritance of growth rate variation. We also present evidence that this defect accounts for its increased frequency of persisters. We further identify the gene responsible for the *HipQ* phenotype as

Significance

Persistence, the phenomenon whereby a small subpopulation of bacterial cells survive sterilization, prolongs antibiotic treatment and contributes to the development of genetic antimicrobial drug resistance (AMR). In this study we performed single-cell tracking of wild-type and high-persister mutant strains of *Escherichia coli* to identify factors that correlate with persistence. We found, as expected, persistence correlated with slow growth, but also with small birth size. We investigated intergenerational (mother–daughter) and intragenerational (sister–sister) phenotypic inheritance of growth parameters and discovered the mutant phenotype was associated with lower levels of phenotypic inheritance and identified the gene responsible, the transcription factor *ydcI*. Targeting pathways involved in persistence could reveal approaches to impeding persistence and the development of AMR.

Author contributions: S.M.H.-W., N.M., Y.H., R.C., A.B., R.J.C., H.L.T., H.W., R.E.B., W.R.J., A.R., and J.M. designed research; S.M.H.-W., N.M., Y.H., R.C., R.E.B., and J.M. performed research; S.M.H.-W., N.M., Y.H., R.C., A.B., R.J.C., H.L.T., H.W., A.R., and J.M. analyzed data; and S.M.H.-W., N.M., Y.H., H.L.T., W.R.J., A.R., and J.M. wrote the paper.

Reviewers: B.B.A., Tufts University; and N.Q.B., Hebrew University of Jerusalem.

The authors declare no competing interest.

Data deposition: Individual sequencing read data for the *E. coli* HipQ mutant and parental strain are publicly available at National Center for Biotechnology Information (NCBI) Biosample, https://www.ncbi.nlm.nih.gov/biosample (accession nos. SAMN13648605 [*E.coli* HipQ mutant strain] and SAMN13648604 [*E. coli* parental strain]).

[1]S.M.H.-W., N.M., and Y.H. contributed equally to this work.

[2]A.R. and J.M. contributed equally to this work.

[3]To whom correspondence may be addressed. Email: j.mcfadden@surrey.ac.uk, william.jacobs@einsteinmed.org, or a.rocco@surrey.ac.uk.

This article contains supporting information online at https://www.pnas.org/lookup/suppl/doi:10.1073/pnas.1914741117/-/DCSupplemental.

First published February 6, 2020.

the recently characterized LysR family transcriptional regulator *ydcI* (14).

Several models of growth and division of cells have been proposed recently (15–18). These include models where cells measure a fixed increase in length between division (i.e., the adder model) (15), sense absolute time [i.e., the timer model (16)], or sense absolute size [i.e., the sizer model (16–18)]. To examine how persistence fits into these paradigms we performed single-cell studies using a microfluidics platform (Fig. 1*A* and *SI Appendix*, Fig. S1*A*) to measure steady state growth and division of individual cells of both the wild-type (WT) and the high-persister *HipQ* mutant (Fig. 1 *A*–*C* and *SI Appendix*, Fig. S1*B*). Growth characteristics (division time T, elongation rate g, size at birth L_0, size at division L_f, and size extension Δ) of both WT and *HipQ* mutant cells were recorded before antibiotic exposure (*SI Appendix*, Table S1). The values of both μ (Fig. 1*B*) and g (Fig. 1*C*) varied widely between generations but, at steady state, appeared constrained in a bounded range of values. We found that cells add an approximately constant length prior to division and hence were behaving consistently with the adder model only (Fig. 1*D*, equation in Fig. 1*E*, and *SI Appendix*, Fig. S1 *C* and *D*). The average value or distribution of measured parameters did not differ significantly between WT and HipQ mutant strains (*SI Appendix*, Table S1 and Fig. S2 *A*–*F*).

We next examined inheritance of phenotypic variation, measuring sister–sister (S–S) correlations within a generation and mother–daughter (M–D) correlations (*SI Appendix*, Tables S2 and S3, respectively) between generations. As found previously (19, 20), M–D correlations of T or Δ were close to zero, indicating that there was virtually no memory of these parameters between mother and daughter cells, but moderate levels of M–D correlations were observed in WT cells on L_0, L_f, and g (*SI Appendix*, Table S3), demonstrating that limited phenotypic information is passed between generations. Despite low M–D correlations on T or Δ, high correlations were found for both these parameters between sisters (*SI Appendix*, Table S2) in WT. Surprisingly, the *HipQ* mutant strain exhibited statistically significant loss of M–D correlations on elongation rate, g, which were less than half the value for the WT (Fig. 2 *C*, *D*, and *F*); also S–S correlations on division time T (Fig. 2 *A*, *B*, and *E*) and (although nonsignificant) elongation rate g were reduced (*SI Appendix*, Table S2). The *HipQ* mutant strain thereby exhibits the phenotype of reduced phenotypic inheritance (RPI) with statistical significance of 0.014 and 0.03 for T and g, respectively, for the HipQ mutant versus WT.

To investigate if and how RPI affects persister formation we characterized persister cells (identified as surviving initial antibiotic exposure but being killed by antibiotic after regrowth; Fig. 1*A* and Movie S1) and their relatives. Persisters tended to be

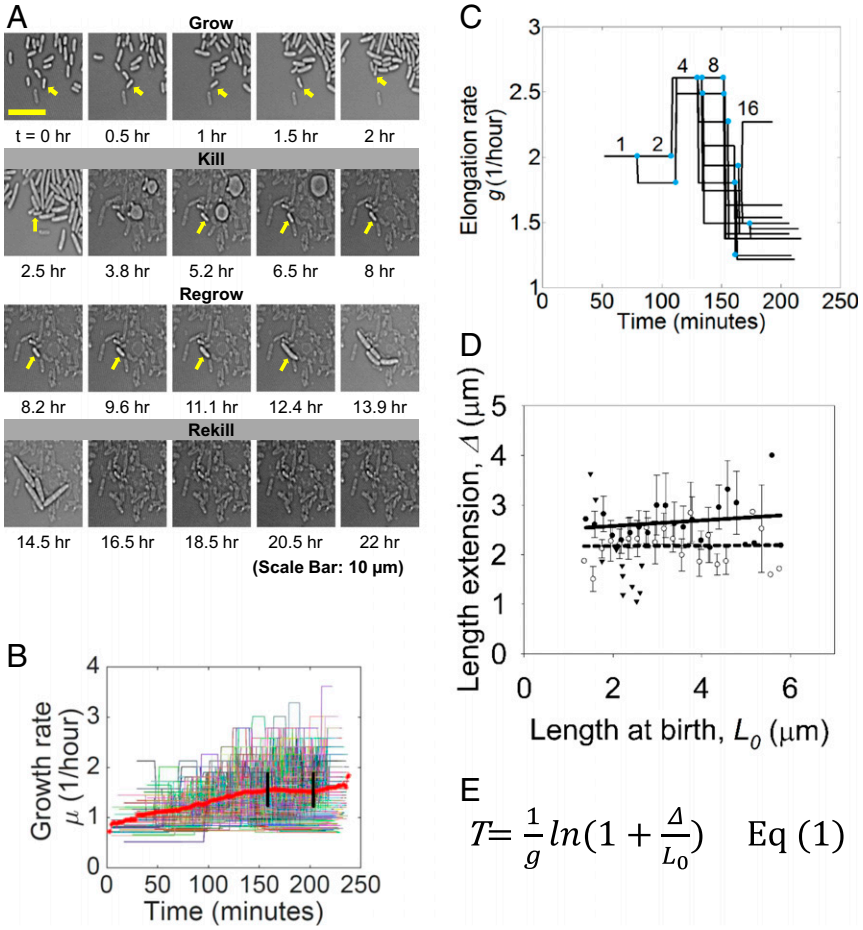

Fig. 1. Single-cell analyses of *E. coli* persisters using microfluidics and image tracking. (*A*) Single-cell data showing persister (yellow arrow). (*B*) WT growth rate (2,172 cells) with black bars indicating steady state and red line indicating mean. (*C*) Elongation rate trajectories. Blue circles indicate divisions, with cell numbers. (*D*) Growth characteristics of cells for the adder model (WT are shown as solid and *HipQ* mutant are shown as clear circles, with persisters' mothers shown as solid triangles). Data represent three experiments (WT = 1,710, mutant = 1,638 cells) with error bars representing $n = 3$. Solid linear fitting line is for WT ($\Delta = (0.0563 \pm 0.0731)L_0 + (2.4646 \pm 0.2730)$), and dashed line is for mutant ($\Delta = (0.0042 \pm 0.0641)L_0 + (2.1654 \pm 0.2355)$). (*E*) Adder model equation.

born with small L_0 (Fig. 3*A*) and grew at slower elongation rates g (Fig. 3*B*), a difference that was statistically significant when compared to the rest of the population and with persister's mothers (Fig. 3 *A* and *B*). Since growth of persisters includes a period of anomalous elongation during exposure to antibiotic it was not possible to measure L_f, T, or Δ; however, the average age

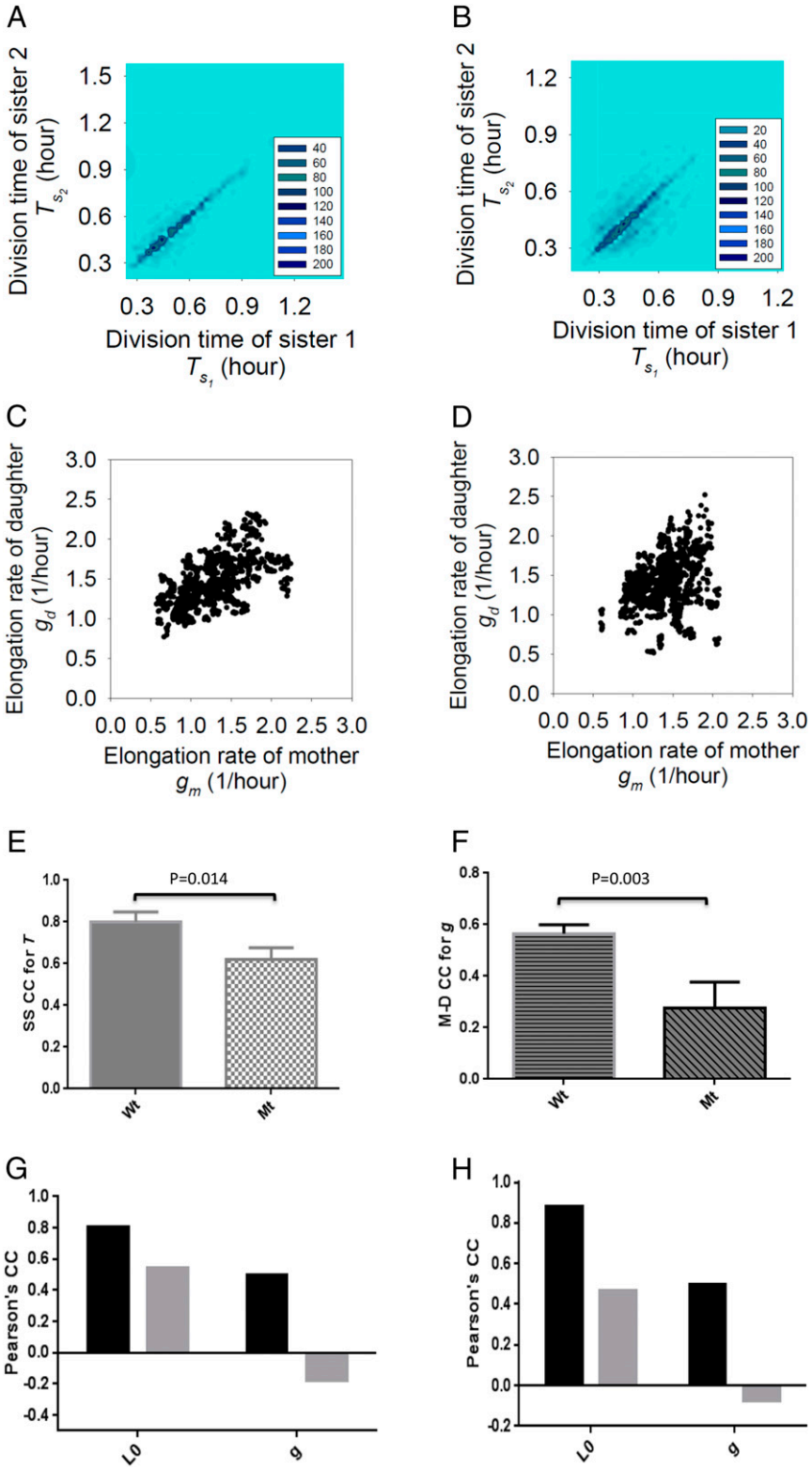

Fig. 2. S–S and M–D growth parameters at the population level. S–S T in (*A*) WT and (*B*) *HipQ* mutant. g between mother and daughter for (*C*) WT and (*D*) mutant. Correlation coefficients (CC) with SDs for *HipQ* mutant for (*E*) S–S T and (*F*) M–D g. Pearson's CC following slow stratification of T and showing L_0 and g between (*G*) S–S and (*H*) M–D with WT in black and mutant in gray. Data represent three independent experiments (WT = 1,710 and mutant = 1,638 cells).

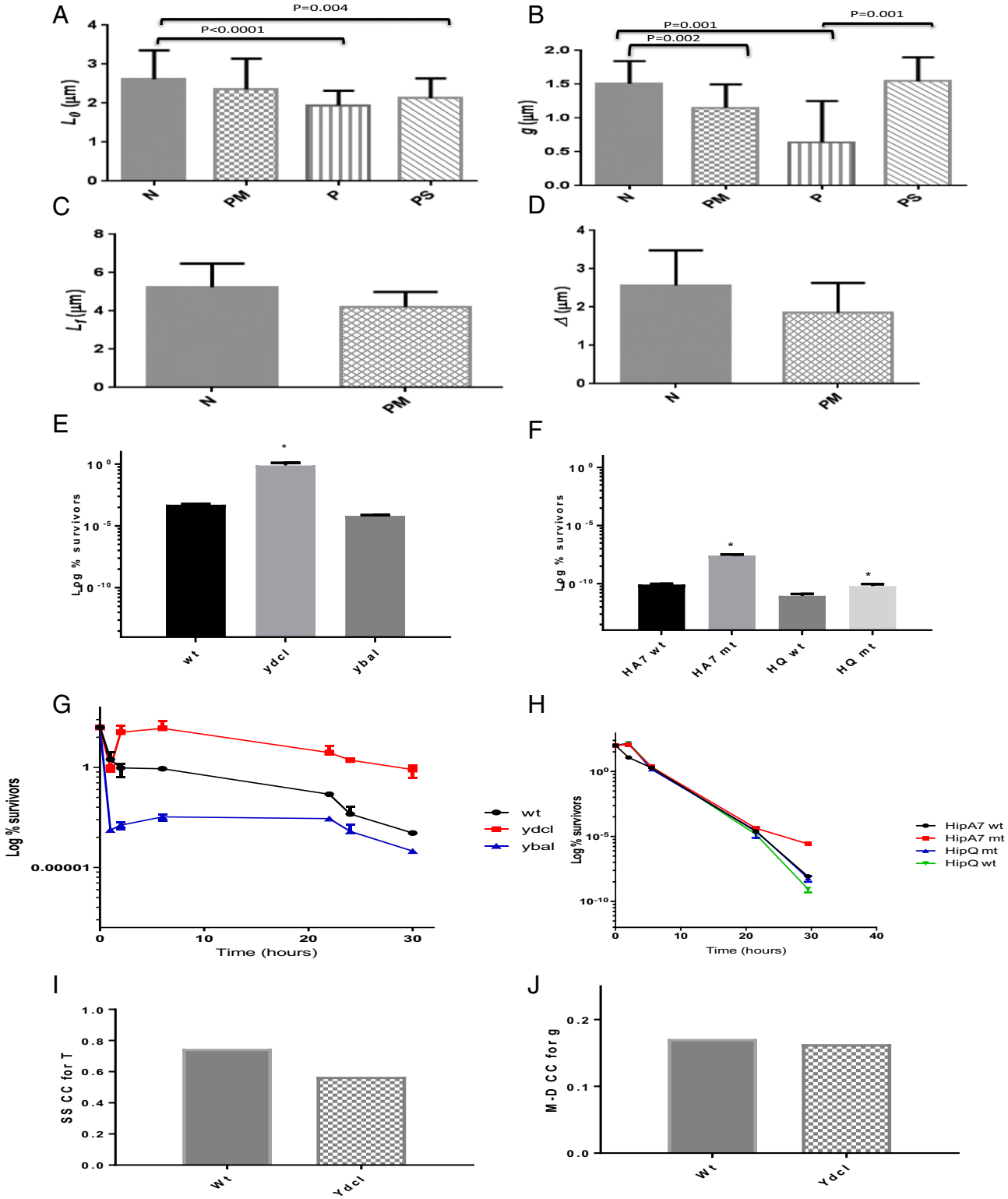

Fig. 3. Persisters are small and slow, with the HipQ mutant gene identified as *ydcI*. (*A*) Size at birth (L_0) and (*B*) elongation rate (g) measurements for normal (N, $n = 1{,}644$), persister's mother (PM, $n = 14$), persister (P, $n = 17$), and persister's sister (PS, $n = 14$) and (*C*) size at division (L_f) and (*D*) Δ for N and PM, from at least 3 individual experiments for N and for over 14 for P, PS, and PM. Statistics were calculated using Student's t test with Welch's correction (absolute effect size of Cohen's standardized mean difference was over 0.9 for all statistically significant comparisons). Percentage survivors at 24 h over time 0 for ampicillin (100 μg/mL) for (*E*) WT, Δ*ydcI*, and Δ*ybaI* and (*F*) *HipA7* mutant and WT and *HipQ* mutant and WT (representative of three experiments). Ampicillin (100 μg/mL) kill curve for (*G*) parental Keio strain, *ydcI*, and *yabI* and (*H*) *hipB* whole-gene knockout mutants ($n = 3$ with SE bars). Correlation coefficients (CC) for *ydcI* mutant ($n = 525$ individual cells) and WT ($n = 624$ cells) for (*I*) S–S T and (*J*) M–D g.

of the persister population, prior to antibiotic addition, was about twice that of the nonpersister population, indicating that their division time is lengthened to compensate for their slower elongation rate, as predicted by the adder model (Fig. 1*E* and *SI Appendix*, Table S4).

The character of persistence thereby appears to be solely due to the persister cell's acquisition of extreme values of L_0 and g. The reduced cell length at birth appears to be phenotypically inherited from the persister cell's mother that tended to be also small at birth and grew at slower rates to achieve a smaller cell size at division (Fig. 3 *C* and *D*) to thereby generate smaller daughters (Fig. 3*A*). We hypothesized that the character of persistence would correlate across sisters; however, surprisingly, given the high degree of correlation for all measured parameters between sisters, the sister of a persister was generally not a persister. However, when cells were stratified according to division time into fast-, medium-, and slow-replicating cells, significantly lower M–D (Fig. 2*G*) and S–S (Fig. 2*H*) correlations on L_0 and g were found for slow-growing *HipQ* mutant cells compared to WT (*SI Appendix*, Fig. S1 *E–H*), indicating that their RPI is enhanced in the slow-growing cells that are the progenitors of persisters, leading to lower sister correlations.

We next hypothesized that reduced M–D phenotypic inheritance of g found in the *HipQ* mutant is responsible for generating its high levels of persisters. To test this hypothesis, we made the assumption that fluctuations in values of g averaged over the cell cycle can be described phenomenologically as a Brownian motion with a friction term mimicking the resistance of g again undergoing large jumps. This corresponds to the Ornstein–Uhlenbeck (OU) process (21), which is the simplest process allowing explicit control of the noise intensity D on g and the correlation time τ of the fluctuations in g. Our assumption was that the *HipQ* mutant is characterized by a smaller correlation time τ than the WT. This model minimally extends equation 1 in Fig. 1 to include dynamics across generations (as it stands, equation 1 in Fig. 1 only relates cell features within the same generation). The capability of this model to give rise to the biphasic behavior of the corresponding killing curves will depend on mechanisms governing the behavior across generations of all other quantities present in equation 1 in Fig. 1, requiring a population model that currently does not exist. We exemplify the qualitative behavior of the OU process for distinct values of the correlation time τ in *SI Appendix*, Fig. S1*K*. The RPI phenotype of the *HipQ* mutant hence caused a slightly longer tail in the distribution of elongation rate g (*SI Appendix*, Fig. S1*K*; although not visible in our population data, most likely hidden in the noise) to thereby generate more slow-growing progenitors of persisters.

To identify the mutation (22) responsible for persistence in the *HipQ* mutant, we whole-genome sequenced the WT and *HipQ* mutant and identified two single-nucleotide polymorphisms (SNPs) with nonsynonymous mutations in genes of unknown function, *ydcI* and *ybal* (23, 24). The SNP in *ydcI* results in a change from nonpolar (alanine) to a charged amino acid (glutamic acid), so is likely to have phenotypic consequences, whereas the *ybal* mutation is a more conservative valine to glycine change. To identify which mutation was responsible for the persister phenotype, we obtained WT and gene deletion strains of each gene from a mutant library (25) and found that the Δ*ydcI* mutant, but not the Δ*ybal* mutant, exhibited high levels of persisters similarly to *HipQ* (Fig. 3 *E–H*), implicating this gene as the cause of the persister phenotype. Single-cell studies carried out on the Δ*ydcI* mutant determined that the mutant strain also exhibited reduced S–S correlations for T similar to the *HipQ* mutant (Figs. 3*I* and 2*E*). Reduced M–D correlations for g were not observed for the Δ*ydcI* mutant; however, the WT (which is a different strain from the *HipQ* WT) had a much lower M–D correlation of g than observed with the *HipQ* WT (Figs. 3*J* and 2*F*). *E. coli ydcI* is a recently characterized LysR family transcriptional regulator with a predicted role in pH homeostasis (14). The trigger for *ydcI* is unknown but may be linked to stress, e.g., pH, and was also previously identified as differentially expressed in a *DosP* (phosphodiesterase) mutant with reduced tryptophanase activity that was associated with increased levels of persistence (26) and in *Salmonella enterica* is required for resistance to acid stress (27).

Discussion

In this study, we have demonstrated that in *E. coli* the *HipQ* high-persister phenotype is caused by a mutation in the gene *ydcI*, which is associated with the phenotype of RPI. This gene affects inheritance of phenotypic variation in bacteria, and this link with RPI remains to be determined in other bacterial species, such as in *Mycobacterium tuberculosis*, where the importance of persisters is undisputed. Persistence in tuberculosis has long been observed in humans and in the mouse model of infection (28–30). Vilcheze and colleagues have established both an in vitro model of tuberculosis persistence (31) and dual reporter mycobacteriophages to observe mycobacterial persister cells (32). Interestingly, enhancing respiration in *M. tuberculosis* via the addition of *N*-acetylcysteine or vitamin C prevented the formation of persisters (31). Other studies have also linked changes in metabolic status to persistence, growth rate, cell size, and asymmetric growth in mycobacteria (28, 33, 34), as in *E. coli* (35, 36). A recent report also links genome replication with cell division in an updated adder model in *E. coli* (37), a subject which is linked to cell cycle control and the inherent asymmetry in highly heterogenous mycobacteria (34). However, the prospective link with RPI remains to be elucidated in tuberculosis or other bacterial infections or when using different antibiotics. In addition, phenotypic variation and its inheritance are of fundamental importance in many other biological phenomena from development, to cancer, epigenetics, and evolution (38, 39). Characterizing the mechanistic link between the *ydcI* gene and RPI may shed light on the underlying mechanisms accounting for phenotypic variation of characters, such as persistence, and may provide ways to target persister cells.

Materials and Methods

Bacterial Strains and Culturing. The *E. coli* HipQ parental WT (MG1655) and *HipQ* mutant strains were obtained from Balaban et al. (8), and the *E. coli* Δ*ydcI* and Δ*ybal* strains plus parental (BW25113) were obtained from the Keio collection, https://cgsc.biology.yale.edu/KeioList.php (22), with the pyub854 vector used for complementation. LB Lennox (Sigma-Aldrich) was used for all liquid growth media, and cultures were maintained at 37 °C plus shaking. Technical agar no. 3 (Sigma-Aldrich) was added to LB for solid media. Ampicillin (Sigma-Aldrich) was used at a final concentration of 100 μg/mL. For batch culture kill curves, aliquots were taken from a culture at optical density (OD) 1.2 to 1.4 and incubated with ampicillin for up to 48 h, at room temperature, with colony-forming units measured at time 0 and then at named intervals.

Sequencing. Whole-genome sequencing was carried out by Edinburgh Genomics. Briefly, the sequencing libraries were prepared using the Nextera XT kit (Illumina) and sequenced on a HiSeq 2500 using the sequencing by synthesis v4 chemistry. The resulting sequences were aligned to the *E. coli* K12 reference genome (U00096.2) using Burrows Wheeler alignment to generate the binary alignment map files. Whole genome sequences are available as BioSample accession nos. SAMN13648604 and SAMN13648605 (https://www.ncbi.nlm.nih.gov/biosample).

Microfluidics Platform. Bacterial cells in log phase (OD of 1.2) were grown as above and diluted 1:5 and filtered five times using a 24 gauge needle before loading into the CellASIC ONIX Microfluidic Platform with B04A Microfluidic Bacteria Plate (with pressurized height of 0.7 μm and at a flow rate of ∼10 μL/hr) as described in ref. 40. Imaging was performed under a Nikon A1M, Eclipse Ti-E confocal miscroscope with an environmental chamber, motorized stage, and perfect focus system (PFS). Automated multiarea imaging with a 40× air objective lens (Nikon Apo λ), a numerical aperture of 0.95 (resolution of ∼0.32 μm) with PFS (resolution of ±25 nm). LB only was used for growth experiments (8 to 10 generation) and for persister cell discovery the stages were as follows: grow, LB for 2 h; kill, LB plus ampicillin (100 μg/mL) for 6 h; regrow, LB for 6 h; and rekill, LB plus ampicillin (100 μg/mL) for 6 h. For the growth period, images were taken every ∼69 s and every 10 mins for the remaining stages.

Image Analysis. A system was developed that is able to track and analyze the cell growth patterns automatically (40). The images were analyzed on a computer equipped with an Intel Core i5 processor and running at 2.2 GHz and the algorithm was implemented using MATLAB. The overall steps were as follows: 1) remove patterns caused by microfluidic platform by subtracting an image of empty microfluidic device from the growth chamber of microfluidic device containing cells; 2) remove artifacts by using a Gaussian filter; 3) detect/segment cells in consecutive frames automatically by using level set algorithm (41) and check segmentation results manually; 4) extract properties of detected cells for next tracking step, such as major axis (length) and centroid position of cells; 5) given the information of detected cells in each image, track cell from one frame to the next to form the trajectories automatically by combining the Kalman filter (42) and Hungarian method (43, 44) and then check tracking results manually; and 6) extract information based on segmentation and tracking results for data analysis, such as division time, length of cells, and genealogy tree (40).

Modeling. We assume that fluctuations of the cell cycle averaged g are described by the OU process:

$$\frac{dg}{dt} = -\frac{1}{\tau}(g-\bar{g}) + \frac{D^{1/2}}{\tau}\xi(t),$$

where $\bar{g}$ is the average g, $\xi(t)$ is Gaussian white noise, D is noise intensity, and τ is the correlation time. The g correlation function results in

$$\langle g(t)g(t')\rangle = \frac{D}{\tau}\exp\left(\frac{t-t'}{\tau}\right),$$

and the stationary probability distribution is

$$p(g) = \frac{1}{\sigma\sqrt{2\pi}}\exp\left(-\frac{(g-\bar{g})^2}{2\sigma^2}\right),$$

with $\sigma^2 = D/\tau$. Reduced M–D correlations in *HipQ* mutant imply a reduced correlation time τ and as a consequence a broader Gaussian distribution. The increased population in the tails of this distribution corresponds to an increased number of persisters.

Data Availability Statement. Keio strains are publicly available at https://cgsc.biology.yale.edu/KeioList.php (25). Single-cell movies are available in Movie S1. Individual sequencing read data for the *E. coli* HipQ mutant and parental strain are publicly available at NCBI Biosample (https://www.ncbi.nlm.nih.gov/biosample) as SAMN13648604 and SAMN13648605, respectively.

ACKNOWLEDGMENTS. This work was funded by the Biotechnology and Biological Sciences Research Council (BBSRC; BB/J002097/1), Royal Society Wolfson Research Merit Award Grant WM130116, National Institutes of Health Grant AI 026170, and the Medical Research Council (MRC; MR/N007328/1). We thank N.Q.B. for the *E. coli HipQ* mutant and WT parental strains and the National BioResource Project (National Institute of Genetics, Japan) for the *E. coli* Keio strains (*ΔydcI*, *ΔybaI*, and WT parental). Whole-genome sequencing and alignment were carried out by Edinburgh Genomics, The University of Edinburgh. Edinburgh Genomics is partly supported through core grants from Natural Environment Research Council (R8/H10/56), MRC (MR/K001744/1), and BBSRC (BB/J004243/1). We also thank the bioimaging suite and Dr. Tom Mendum at the University of Surrey.

1. G. L. Hobby, E. Meyer, E. Chaffee, Observations on the mechanism of action of penicillin. *Exp. Biol. Med.* **50**, 281–285 (1942).
2. J. Bigger, Treatment of Staphylococcal infections with penicillin by intermittent sterilisation. *Lancet* **244**, 497–500 (1944).
3. N. Dhar, J. D. McKinney, Microbial phenotypic heterogeneity and antibiotic tolerance. *Curr. Opin. Microbiol.* **10**, 30–38 (2007).
4. J. W. Costerton, P. S. Stewart, E. P. Greenberg, Bacterial biofilms: A common cause of persistent infections. *Science* **284**, 1318–1322 (1999).
5. N. Sufya, D. G. Allison, P. Gilbert, Clonal variation in maximum specific growth rate and susceptibility towards antimicrobials. *J. Appl. Microbiol.* **95**, 1261–1267 (2003).
6. D. Leszczynska, E. Matuszewska, D. Kuczynska-Wisnik, B. Furmanek-Blaszk, E. Laskowska, The formation of persister cells in stationary-phase cultures of *Escherichia coli* is associated with the aggregation of endogenous proteins. *PLoS One* **8**, e54737 (2013).
7. H. Luidalepp, A. Jõers, N. Kaldalu, T. Tenson, Age of inoculum strongly influences persister frequency and can mask effects of mutations implicated in altered persistence. *J. Bacteriol.* **193**, 3598–3605 (2011).
8. N. Q. Balaban, J. Merrin, R. Chait, L. Kowalik, S. Leibler, Bacterial persistence as a phenotypic switch. *Science* **305**, 1622–1625 (2004).
9. N. Q. Balaban *et al.*, Definitions and guidelines for research on antibiotic persistence. *Nat. Rev. Microbiol.* **17**, 441–448 (2019).
10. H. S. Moyed, S. H. Broderick, Molecular cloning and expression of *hipA*, a gene of *Escherichia coli* K-12 that affects frequency of persistence after inhibition of murein synthesis. *J. Bacteriol.* **166**, 399–403 (1986).
11. S. B. Korch, T. A. Henderson, T. M. Hill, Characterization of the hipA7 allele of *Escherichia coli* and evidence that high persistence is governed by (p)ppGpp synthesis. *Mol. Microbiol.* **50**, 1199–1213 (2003).
12. E. Rotem *et al.*, Regulation of phenotypic variability by a threshold-based mechanism underlies bacterial persistence. *Proc. Natl. Acad. Sci. U.S.A.* **107**, 12541–12546 (2010).
13. A. Rocco, A. M. Kierzek, J. McFadden, Slow protein fluctuations explain the emergence of growth phenotypes and persistence in clonal bacterial populations. *PLoS One* **8**, e54272 (2013).
14. Y. Gao *et al.*, Systematic discovery of uncharacterized transcription factors in Escherichia coli K-12 MG1655. *Nucleic Acids Res.* **46**, 10682–10696 (2018).
15. M. Osella, E. Nugent, M. Cosentino Lagomarsino, Concerted control of *Escherichia coli* cell division. *Proc. Natl. Acad. Sci. U.S.A.* **111**, 3431–3435 (2014).
16. L. Robert *et al.*, Division in Escherichia coli is triggered by a size-sensing rather than a timing mechanism. *BMC Biol.* **12**, 17 (2014).
17. M. Campos *et al.*, A constant size extension drives bacterial cell size homeostasis. *Cell* **159**, 1433–1446 (2014).
18. S. Taheri-Araghi *et al.*, Cell-size control and homeostasis in bacteria. *Curr. Biol.* **25**, 385–391 (2015).
19. D. J. Kiviet *et al.*, Stochasticity of metabolism and growth at the single-cell level. *Nature* **514**, 376–379 (2014).
20. P. Wang *et al.*, Robust growth of *Escherichia coli*. *Curr. Biol.* **20**, 1099–1103 (2010).
21. C. W. Gardiner, *Handbook of Stochastic Methods* (Springer, Dallas, TX, 1985).
22. J. S. Wolfson, D. C. Hooper, G. L. McHugh, M. A. Bozza, M. N. Swartz, Mutants of *Escherichia coli* K-12 exhibiting reduced killing by both quinolone and beta-lactam antimicrobial agents. *Antimicrob. Agents Chemother.* **34**, 1938–1943 (1990).
23. S. M. Hingley-Wilson, J. J. McFadden, *E. coli* parental strain. National Center for Biotechnology Information. https://www.ncbi.nlm.nih.gov/biosample/?term=SAMN13648604. Deposited 20 December 2019.
24. S. M. Hingley-Wilson, J. J. McFadden, *E.coli* HipQ mutant strain. National Center for Biotechnology Information. https://www.ncbi.nlm.nih.gov/biosample/?term=SAMN13648605. Deposited 20 December 2019.
25. T. Baba *et al.*, Construction of *Escherichia coli* K-12 in-frame, single-gene knockout mutants: The Keio collection. *Mol. Syst. Biol.* **2**, 2006.0008 (2006).
26. B. W. Kwan, D. O. Osbourne, Y. Hu, M. J. Benedik, T. K. Wood, Phosphodiesterase DosP increases persistence by reducing cAMP which reduces the signal indole. *Biotechnol. Bioeng.* **112**, 588–600 (2015).
27. M. E. Jennings *et al.*, Characterization of the *Salmonella enterica* serovar Typhimurium *ydcI* gene, which encodes a conserved DNA binding protein required for full acid stress resistance. *J. Bacteriol.* **193**, 2208–2217 (2011).
28. C. Vilchèze, W. R. Jacobs, Jr., The isoniazid paradigm of killing, resistance, and persistence in *Mycobacterium tuberculosis*. *J. Mol. Biol.* **431**, 3450–3461 (2019).
29. D. Mitchison, G. Davies, The chemotherapy of tuberculosis: Past, present and future. *Int. J. Tuberc. Lung Dis.* **16**, 724–732 (2012).
30. R. M. McCune, F. M. Feldmann, H. P. Lambert, W. McDermott, Microbial persistence. I. The capacity of tubercle bacilli to survive sterilization in mouse tissues. *J. Exp. Med.* **123**, 445–468 (1966).
31. C. Vilchèze *et al.*, Enhanced respiration prevents drug tolerance and drug resistance in *Mycobacterium tuberculosis*. *Proc. Natl. Acad. Sci. U.S.A.* **114**, 4495–4500 (2017).
32. P. Jain *et al.*, Dual-reporter mycobacteriophages (Φ2DRMs) reveal preexisting *Mycobacterium tuberculosis* persistent cells in human sputum. *MBio* **7**, e01023-16 (2016).
33. M. Priestman, P. Thomas, B. D. Robertson, V. Shahrezaei, Mycobacteria modify their cell size control under sub-optimal carbon sources. *Front. Cell Dev. Biol.* **5**, 64 (2017).
34. M. M. Logsdon, B. B. Aldridge, Stable regulation of cell cycle events in mycobacteria: Insights from inherently heterogeneous bacterial populations. *Front. Microbiol.* **9**, 514 (2018).
35. N. S. Hill, P. J. Buske, Y. Shi, P. A. Levin, A moonlighting enzyme links *Escherichia coli* cell size with central metabolism. *PLoS Genet.* **9**, e1003663 (2013).
36. E. J. Stewart, R. Madden, G. Paul, F. Taddei, Aging and death in an organism that reproduces by morphologically symmetric division. *PLoS Biol.* **3**, e45 (2005).
37. G. Micali, J. Grilli, J. Marchi, M. Osella, M. Cosentino Lagomarsino, Dissecting the control mechanisms for DNA replication and cell division in *E. coli*. *Cell Rep.* **25**, 761–771.e4 (2018).
38. A. Brock, H. Chang, S. Huang, Non-genetic heterogeneity—A mutation-independent driving force for the somatic evolution of tumours. *Nat. Rev. Genet.* **10**, 336–342 (2009).
39. J. Trott, K. Hayashi, A. Surani, M. M. Babu, A. Martinez-Arias, Dissecting ensemble networks in ES cell populations reveals micro-heterogeneity underlying pluripotency. *Mol. Biosyst.* **8**, 744–752 (2012).
40. Y. Hu *et al.*, Trajectory energy minimization for cell growth tracking and genealogy analysis. *R. Soc. Open Sci.* **4**, 170207 (2017).
41. S. Osher, J. A. Sethian, Fronts propagating with curvature-dependent speed: Algorithms based on Hamilton-Jacobi formulations. *J. Comput. Phys.* **79**, 12–49 (1988).
42. R. E. Kalman, A new approach to linear filtering and prediction problems. *J. Fluids Eng.* **82**, 35–45 (1960).
43. R. Kaucic, G. Brooksby, J. Kaufhold, A. Hoogs, "A unified framework for tracking through occlusions and across sensor gaps" in *Computer Vision and Pattern Recognition. EEE Computer Society Conference*, vol. 1, pp. 990-997 (2005).
44. C. Stauffer, "Estimating tracking sources and sinks" in *Computer Vision and Pattern Recognition Workshop. CVPRW'03 Conference*, vol. 4, pp. 35–35 (2003).